Neurosci. Bull. March, 2020, 36(3):217–229
https://doi.org/10.1007/s12264-019-00427-z

www.neurosci.cn
www.springer.com/12264

ORIGINAL ARTICLE

Projection from the Anterior Cingulate Cortex to the Lateral Part of Mediodorsal Thalamus Modulates Vicarious Freezing Behavior

Chaowen Zheng[1,2] · Yanwang Huang[1,2] · Binshi Bo[1] · Lei Wei[1] · Zhifeng Liang[1] · Zuoren Wang[1,2,3]

Received: 11 March 2019 / Accepted: 26 May 2019 / Published online: 17 September 2019

Abstract Emotional contagion, a primary form of empathy, is present in rodents. Among emotional contagion behaviors, social transmission of fear is the most studied. Here, we modified a paradigm used in previous studies to more robustly assess the social transmission of fear in rats that experienced foot-shock. We used resting-state functional magnetic resonance imaging to show that foot-shock experience enhances the regional connectivity of the anterior cingulate cortex (ACC). We found that lesioning the ACC specifically attenuated the vicarious freezing behavior of foot-shock-experienced observer rats. Furthermore, ablation of projections from the ACC to the mediodorsal thalamus (MDL) bilaterally delayed the vicarious freezing responses, and activation of these projections decreased the vicarious freezing responses. Overall, our results demonstrate that, in rats, the ACC modulates vicarious freezing behavior *via* a projection to the MDL and provide clues to understanding the mechanisms underlying empathic behavior in humans.

Keywords Rat · Empathy · Vicarious freezing · Neuronal circuit

✉ Zuoren Wang
zuorenwang@ion.ac.cn

[1] Institute of Neuroscience, State Key Laboratory of Neuroscience, CAS Center for Excellence in Brain Science and Intelligence Technology, Chinese Academy of Sciences, Shanghai 200031, China

[2] University of Chinese Academy of Sciences, Beijing 100049, China

[3] School of Future Technology, University of Chinese Academy of Sciences, Beijing 100049, China

Introduction

Empathy refers to the capability of a subject to stand in another individual's situation and experience the feelings of the latter [1]. It is a sophisticated psychological process vital for individuals to live in society. In addition, abnormalities in this ability are closely associated with mental diseases, such as autism spectrum disorder [2, 3] and schizophrenia [4–6]. Thus, defining the neuronal mechanisms underlying empathy could enable understanding and lead to cures for psychiatric disorders. Currently, these mechanisms in humans remain unknown, in part due to limited research methods.

Initially, researchers defined empathy as unique to humans and apes [7, 8]. Now, increasing evidence has shown that empathy is evolutionarily conserved from rodents to humans [1, 9]. Although advanced empathic behaviors such as perspective-taking have not been defined in rodents, many studies support the idea that rodents exhibit emotional contagion [10, 11], a primary form of empathic behavior. In the hierarchy of empathic behaviors, emotional contagion refers to an individual's ability to unconsciously mimic the emotional state of a conspecific [7] and is thought to be a fundamental component of advanced empathy [12, 13]. Examples of emotional contagion include the contagion of a baby's cry [14] and the social transmission of fear [15, 16]. Thus, understanding the mechanisms of emotional contagion in simpler animals could shed light on the neuronal basis of advanced empathy in humans.

To date, behavioral studies have revealed a variety of primary empathy behaviors in rodents, such as social buffering [17], social analgesia [18], and social transmission of fear. Among these, the last has been most studied in rodents, mainly using the paradigm of observational fear

established by Shin and colleagues [11]. Observational fear tasks evaluate the social transmission of fear by detecting the vicarious behavior of an observer (OS) when a demonstrator (DS) suffers distress (such as foot-shock, a mild electric shock administered to the feet of rats), but some studies have reported that since the OS must observe the foot-shock response of the DS in real time, the resulting vicarious behavior likely includes a startle-induced component [19]. However, in another paradigm reported by Kim *et al*. [20], the OS performs a vicarious response simply by observing the emotional state of the DS, without a startle-induced component. Thus, in the present study, we used Kim's behavioral paradigm to further explore the potential mechanisms.

The neuronal substrates underlying the social transmission of fear remain largely unknown. Previous studies have shown that the anterior cingulate cortex (ACC) modulates vicarious freezing behavior in a paradigm of observational fear [15], since current-injection stimulation or lesion of the ACC respectively increased or decreased vicarious freezing. Shin's lab also found that optogenetic activation or inhibition of somatostatin-positive neurons in the ACC respectively decreased or increased observational fear [21]. Several studies have also reported that the neuropeptide oxytocin modulates empathy-related behaviors in humans [22–24] as well as social behavior-like observational fear in rodents [25]. In particular, intranasal administration of oxytocin increases ACC neuronal activity and vicarious freezing behavior in mice [25]. Since the ACC appears to be closely associated with vicarious freezing behavior, and the capacity for empathy is strongly associated with personal experience, especially unpleasant experience, in humans [26], it is important to determine whether foot-shock experience enhances vicarious freezing behavior by increasing ACC activity. If so, this would be conducive to further understanding the potential neuronal mechanism underlying unpleasant-experience-induced empathy disorder.

Among the structures downstream of the ACC, the lateral part of the mediodorsal thalamus (MDL) has been reported to participate in observational fear learning [15]. In addition, since the ACC is close to and partially overlaps with the medial prefrontal cortex (mPFC), and disconnection of the mPFC from the MD is associated with dysfunction of working memory [27–29], reduced cognitive flexibility [30–32], and especially schizophrenia [33–36] (which is accompanied by abnormal empathy [4–6]), it is of great interest to explore the function of the neuronal projection between the ACC and the MD in the process of vicarious freezing behavior.

We therefore set out to determine which brain region was activated after footshock-experience and its role in footshock-experienced vicarious freezing behavior. We also want to explore function of ACC and the projection from ACC to MDL in vicarious freezing behavior.

Experimental Procedures

Animals

We used a total of 346 wild-type male Sprague–Dawley rats weighing 300 g–450 g each. Among them, 164 were used for behavioral tests, 15 for fMRI scanning, 60 for the chemical lesion study, 2 for neuronal circuit-tracing, 41 for the caspase3 apoptosis study, 2 for patch-clamp recording, and 62 for optogenetic manipulation. All rats were reared in pairs in exhaust-ventilated cages under a 12 h/12 h light/dark cycle. Water and food were supplied *ad libitum*. The use of animals bred for and manipulated in this study was approved by the Animal Care and Use Committee of the Institute of Neuroscience, Chinese Academy of Sciences, and experiments were performed in accordance with the guidelines of the Ministry of Science and Technology of the People's Republic of China for the Care and Use of Laboratory Animals.

Establishment of the Paradigm

Social Transmission of Fear Under Kim's Paradigm

Under Kim's paradigm, rats paired in the same cage served as respective DS and OS. On day 1, the DS underwent 10 trials of classical fear conditioning training in a closed electrical shock box: in each trial, a conditioned stimulus (sound cue, 5 kHz) was presented persistently for 20 s, accompanied in the last second by an unconditioned foot shock (1 s, 2 mA). Both stimuli ended simultaneously. The intertrial interval was 1 min and the session ended 2 min after the last foot shock. OSs were divided into naïve and foot-shock-experienced groups. The latter underwent the following foot-shock paradigm before the test day. After 3 min of adaption to the shock cage, one foot shock was delivered (1 s, 2 mA), followed by another 3 min later. By contrast, naïve OSs did not experience a foot shock prior to the test day. On day 2, DSs and OSs were placed in a new open box, and after 1 min, the conditioned stimulus (5 kHz tone) was presented persistently for 7 min to test the responses of DSs and OSs.

Fear conditioning learning was established in a stainless-steel shock box measuring 27 × 28 × 30 cm^3. The floor consisted of 18 stainless-steel tubes (outer diameter, 5 mm) and the ceiling was a transparent acrylic plate. The open box used to test the social transmission of fear was 35 × 36 × 40 cm^3 and made of white acrylic plates. The sound cue was played using a full-frequency-range

loudspeaker (FR89EX; Fountek Electronics Co., Ltd, Jiaxing, China), and an electric shock was delivered by a constant current stimulator (Anilab Software and Instruments Co., Ltd, Ningbo, China). Both the sound cue and foot shock stimuli were controlled by Anilab software.

Social Transmission of Fear Under an Optimized Paradigm

In our modified paradigm, DSs underwent fear-conditioning training on days 1 and 2 (10 trials on each day), while OSs received foot shocks twice on day 2 only, and the social transmission of fear was tested on day 3. Other conditions were the same as in Kim's paradigm. All the behavioral tests of social transmission shown in Figs. 3, 4 and 5 used this modified paradigm.

Pharmacological Lesioning

In the lesion studies, general anesthesia was maintained by pentobarbital sodium (80 mg/kg, i.p.). Atropine sulfate (0.05 mg/kg, i.p.) was administered to inhibit mucus secretion, which hinders breathing. Glass electrodes for ibotenic acid (IBO) injection (5 mg/mL, Sigma, St. Louis, MO) were pulled on a P97 system (Sutter Instrument Co., Novato, USA). The Pico III system (Parker Hannifin, Mayfield Heights, OH) was used to pump IBO (1 μL) bilaterally into the ACC (AP, +1.35 mm; ML, 0.60 mm; DV, 2.4 mm). After suturing, gentamycin (5 mg/kg, i.p.) was administered for one week to minimize infection. After 1 week of recovery, the social transmission of fear was tested using our optimized paradigm. The retrieval test occurred on the second day after fear conditioning training in the same box used for the social transmission of fear. The experimental settings and procedures were the same as in the social transmission of fear test on day 3.

Caspase 3 Ablation

For virus injection, the procedures followed the same sequence as for stereotactic injection in the pharmacological experiment. After 3 weeks of virus expression, the social transmission of fear was tested using our optimized paradigm.

Optogenetic Activation

For virus injection, the procedures followed the same sequence as for the stereotactic injection in the pharmacological experiment. Before implantation of the optical fibers into the MDL (AP, − 2.55 mm; ML, 1.00 mm; DV, 4.50 mm), three bone screws were fixed to the rat's skull and acrylic dental cement was used to stabilize the fibers. Gentamycin was administered as above. Three weeks after virus injection, the rats underwent behavioral tests. The social transmission of fear test was the same as before. Blue light was delivered to the MDL of the virus-injected rats throughout the test period. The lasers used to deliver blue light (473 nm, BL473T3-050FC) were from Shanghai Laser & Optics Century Co., Ltd. The power intensity was set to 5 mW at the tips of the fibers and confirmed using a Fiber Optic Power Meter (Thorlabs, Inc., Newton, NJ). The frequency of laser stimulation (controlled by Anilab software) in the behavioral tests was set to 20 Hz with a 25-ms pulse-width.

To establish fear conditioning and for the fear memory retrieval test, the procedure was the same as in the pharmacological experiment. Locomotion was recorded. The frequency, duration, and intensity of the blue light stimuli were the same as above. An optical fiber commutator was used to prevent twisting of the cable.

Open Field Test

For virus injection and implantation of the optical fibers, the procedures were the same as for stereotactic injection in the pharmacological experiment and social transmission of fear with optogenetic activation part.

In the open field test, rats were placed in a box measuring 54 × 40 × 38 cm^3. On day 1, locomotion was recorded for 30 min using the Cineplex (Plexon Inc., Hong Kong, China) system in the absence of laser stimulation with the fiber cable attached. However, on day 2 the light pulses and locomotion were recorded. The light frequency, duration, and intensity were set the same as the parameters in optogenetic activation part.

Video Tracking and Analysis

Rats were marked with different colors, and their locomotion was tracked as above and saved in text files. Freezing behavior was defined as when an animal did not move (except for spontaneous respiration) for at least 2 s. Huddling time was defined as the period when two rats were within huddling distance. Statistics relevant to freezing and huddling times and locomotor velocity were processed in MATLAB (MathWorks, Natick, MA).

Resting-State Functional Magnetic Resonance Scanning (rs-fMRI) and Image Processing

Ten male Sprague-Dawley rats in the footshock-experienced group and 5 in the control group were anesthetized with isoflurane (5% for induction, 0.5% for maintenance) and paralyzed with dexmedetomidine (0.03 mg/kg bolus, 0.015 mg/kg per hour continuous subcutaneous infusion).

Respiration rate, rectal temperature, O_2 saturation, and heart rate were maintained within the following ranges: 40–60 breaths/min, 36 °C–37 °C, 98%–100%, and 200–300 beats/min. MRI data were acquired using a small-animal 9.4T MR system (Bruker BioSpec 94/30, Ettlingen, Germany) equipped with a 2 × 2 phased array surface receiver coil. T2 RARE anatomical images were acquired with a repetition time/echo time = 3735 ms/33 ms, field of view = 30 × 30 mm^2, matrix size = 256 × 256, slice thickness 0.6 mm, number of slices 35, and number of averages 1. Gradient-echo echo-planar imaging (GE-EPI) data were acquired with a repetition time/echo time/flip angle = 1000 ms/13 ms/55°, 600 repetitions, matrix dimensions = 80 × 67, in-plane voxel dimensions of 375 × 373 μm^2, and slice thickness 0.6 mm.

Functional images were processed using scripts custom-written in MatLab and SPM12 (http://www.fil.ion.ucl.ac.uk/spm/). The preprocessing included the following main steps. (1) EPI images were converted from Bruker format to NIFTI format (nominal voxel size enlarged 10 times to facilitate image processing in SPM). (2) Realignment: the first 5 volumes were discarded to minimize relaxation-related signal changes and then realigned for motion correction. (3) Spatial normalization: the realigned EPI images were co-registered to the rat's own T2 anatomical images, which were normalized to a rat brain template [37]. (4) The normalized images were band-pass filtered (0.001 Hz–0.1 Hz) and the whole brain signal and the six motion parameters were regressed. (5) Regional homogeneity (ReHo) calculation: Kendall's coefficient was calculated to determine the degree of regional synchronization, including the 27 pixels of the fMRI time courses [38]. Individual ReHo maps were generated voxel-wise for all groups. (6) Smoothing: spatial smoothing was applied with a 0.8-mm full-width at half-maximum Gaussian kernel.

Virus

Recombinant adeno-associated virus (AAV) vectors of serotype 9 were packaged by Shanghai Taitool Bioscience Co. Ltd. Viral titers were 1.32 × 10^{13} particles/mL for AAV-hSyn-hChR2-EGFP-ER2-WPRE-PolyA, 1.61 × 10^{13} particles/mL for AAV-hSyn-eGFP-3Flag-WPRE-SV40pA, 1.16 × 10^{13} particles/mL for AAV-hSyn-FLEX-tdTomato-WPRE-bGHpA, 2.03 × 10^{13} particles/mL for AAV-CAG-DIO-taCasp3-TEVp, 1.60 × 10^{13} particles/mL, and 1.82 × 10^{13} particles/mL for AAV-CMV_bGI-Cre-EGFP. The viruses were injected in a volume of 1 μL on each side.

Perfusion and Histology

After the rats were deeply anesthetized (as above), they were perfused transcardially with phosphate-buffered saline (PBS) until the liver began to turn yellow, and then the PBS was replaced by 4% formaldehyde. After the tail became stiff, the brain was removed and post-fixed in 4% formaldehyde for 12 h, followed by incubation in 30% sucrose. When the brain sank, 50 μm coronal sections were cut on a freezing microtome.

For histology, we performed 4′,6-diamidino-2-phenylindole (DAPI, Sigma) staining. Sections were washed 3 times in PBS for 5 min and then incubated for 5 min with DAPI. After two 5-min PBS washes, sections were mounted with 75% glycerin. Images were acquired using an Olympus VS120 High Throughput fluorescent imaging system (Shinjuku, Tokyo, Japan) with a 10 × air objective.

Statistics

Two-way repeated measures analysis of variance (ANOVA) was used to analyze the differences in ReHo values between two groups, and the interaction effects (time and condition) F map calculated in SPM12 was used to analyze the differences in ReHo values between two groups. Multiple comparison correction was done using the AlphaSim function (corrected $P < 0.05$) in REST software [39]. Student's *t*-test was used to further analyze the interaction type in brain areas showing significant interaction effects.

Results

Behavioral Paradigm

To define the neuronal mechanisms underlying the social transmission of fear in rats, the overall experimental design is shown in Fig. 1. We first applied a paradigm based on that of Kim *et al.* [20] (Fig. 2A). Cage-mates were randomly divided into DS and OS groups. On day 1, the DS underwent classical fear conditioning training, in which a foot-shock (unconditioned stimulus) was associated with

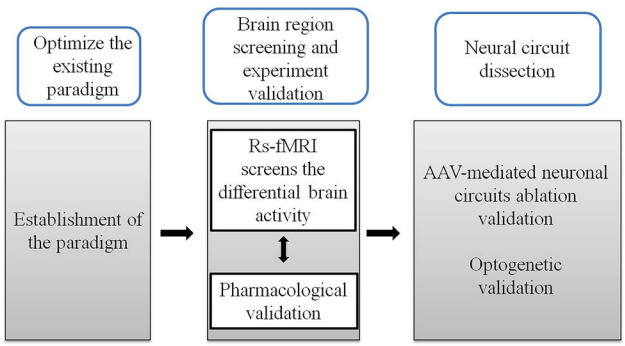

Fig. 1 Experimental design. Schematic of the experimental design of the present study.

a sound cue (conditioned stimulus). OS rats either experienced foot-shock twice (2 mA, 1 s, as the experience group (EP)) or were left untreated (naïve, NA). The behavioral responses of OSs were tested on day 2, when both DSs and OSs were placed together in pairs and continuously exposed to the conditioned stimulus in a new context. To confirm that the behavioral response of OSs was indeed caused by DSs, the control group (Ctrl) was set to test the behavioral response of EP OSs to the naïve DSs. Compared with the NA and Ctrl groups, the huddling time of DSs and OSs of the EP group was significantly increased (Fig. 2B; $n = 12$ pairs/group, $P < 0.05$ EP *vs* NA, and

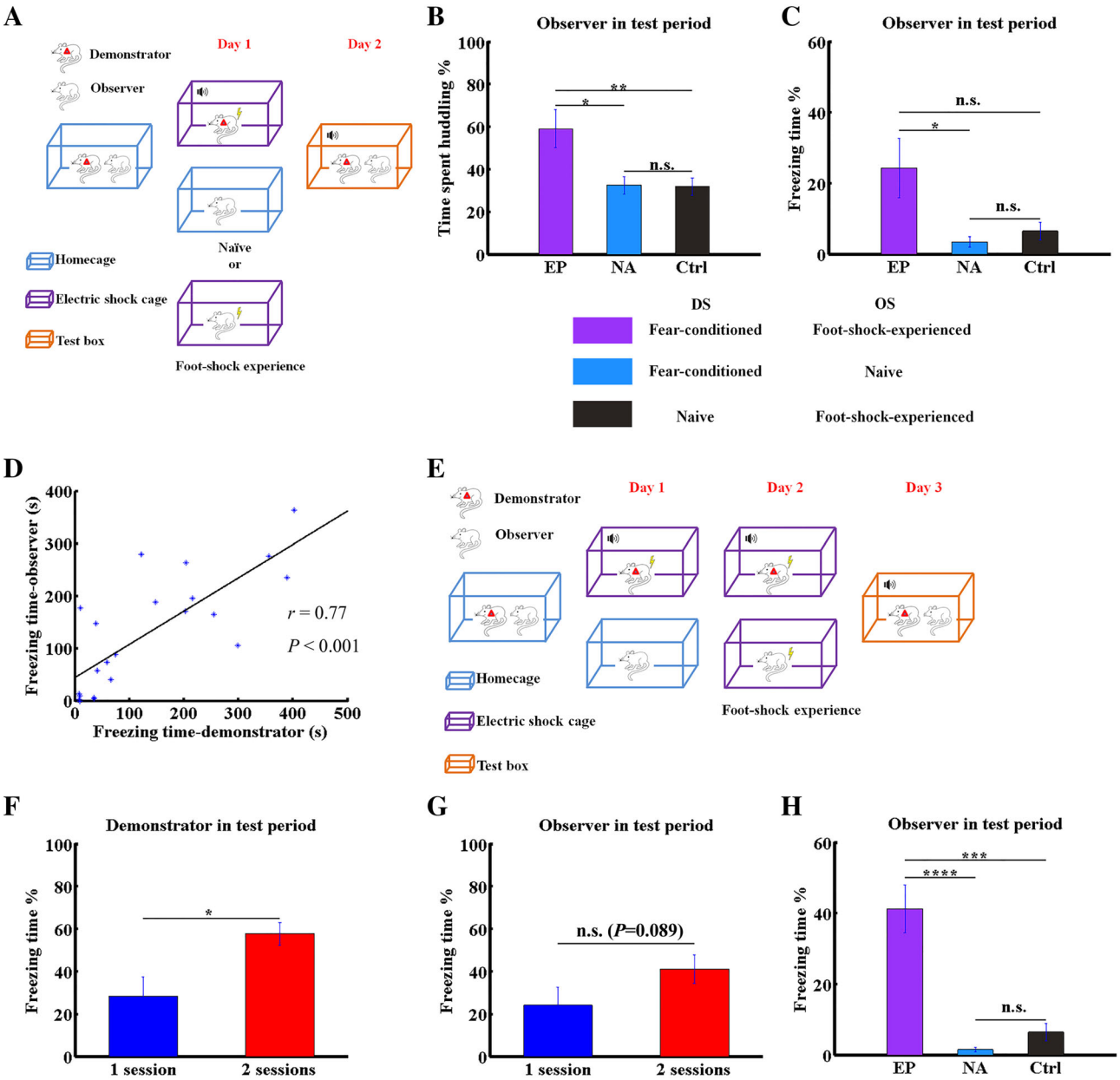

Fig. 2 Behavioral paradigm modification. **A** Schematic of the paradigm adapted from Kim *et al.* [20]. Different colored boxes represent different experimental contexts. **B**, **C** Percentage of huddling (**B**) and freezing (**C**) times of OSs in the indicated groups. **D** Correlation of freezing times between fear conditioned DSs and foot-shock-experienced OS cage-mates ($n = 22$, $P < 0.001$, Student's *t*-test). **E** Schematic showing our modified paradigm. **F** Percentage freezing time of DSs in the EP group in Kim's (1 session) and our modified paradigm (2 sessions) on the test day ($n = 12$, $P < 0.05$, non-parametric rank-sum test). **G** Percentage freezing time of OSs in the EP group in Kim's (1 session) and our modified paradigm (2 sessions) on the test day ($n = 12$, $P = 0.089$, non-parametric rank-sum test). **H** Percentage freezing time of OSs in the EP, NA, and Ctrl groups ($n = 12$, $P < 0.0001$ for EP *vs* NA and $P < 0.001$ for EP *vs* Ctrl). Data are shown as the mean ± SEM; asterisks represent the level of significance: $^{*}P < 0.05$, $^{**}P < 0.01$, $^{***}P < 0.001$, n.s., not significant, non-parametric rank-sum test.

$P < 0.01$ EP *vs* Ctrl, non-parametric rank-sum test), indicating that foot-shock experience by the OS enhanced the social transmission of fear. However, unlike the findings of Kim *et al*. [20], we found that under our experimental conditions, the level of vicarious freezing of OSs tended to increase relative to the Ctrl group (Fig. 2C), but this apparent increase was not statistically significant ($n = 12$ pairs/group, $P = 0.13$, non-parametric rank-sum test). To find the reason for the inconsistency between our and Kim's results, we performed correlation analysis of total freezing time between fear-conditioned DSs and their foot-shock-experienced OS cage-mates in the test period. The results revealed a positive correlation between the freezing time of DSs and OSs (Fig. 2D; $n = 22$, $r = 0.77$, $P < 0.001$, Student's *t*-test). This indicated that the low vicarious freezing level of OSs was probably due to the low freezing level of DSs. As expected, only 5 out of 12 DSs in the EP group exhibited obvious freezing behavior (> 100 s) in the test period on day 2 under the conditions of Kim's paradigm. These results suggested that unstable performance by DSs may explain why we did not find significant vicarious freezing responses in OSs.

To achieve more robust vicarious freezing behavior, we modified the paradigm by increasing the number of sessions of fear conditioning training of DSs to two and then moving the OS foot-shock experience to day 2 (Fig. 2E *vs* Fig. 2A). Using this paradigm, we found that the freezing level of DSs in the EP group in the test period was significantly greater than that under Kim's paradigm (Fig. 2F; $n = 12$ pairs for each of the 1-session and 2-sessions groups, $P < 0.05$, non-parametric rank-sum test), and 10 out of 12 DSs in our modified paradigm exhibited obvious freezing behavior (> 100 s). In our modified paradigm, the level of vicarious freezing behavior of OSs in the EP group showed a tendency to increase compared with that under Kim's paradigm (Fig. 2G; $n = 12$ pairs for each of the 1-session and 2-sessions groups, $P = 0.089$, non-parametric rank-sum test). Furthermore, under the modified paradigm, the level of vicarious freezing in OSs in the EP group was significantly higher than those in the NA and Ctrl groups (Fig. 2H; $n = 12$ pairs/group, $P < 0.0001$ for EP *vs* NA and $P < 0.001$ for EP *vs* Ctrl, non-parametric rank-sum test). These results support the conclusion that our optimized paradigm is more stable for studies of the potential neuronal mechanisms of experience-dependent vicarious freezing behavior.

Foot-Shock Experience Elevates Basic ACC Activity

We next asked whether foot-shock experience modulates the activity of a specific brain region. To do so, we performed rs-fMRI and computed which brain region exhibited significant changes after foot-shock experience. The control and foot-shock-experienced groups underwent fMRI scanning on days 1 and 2, although the latter underwent foot-shock on the night of day 1 (Fig. 3A). We used the ReHo algorithm, as it reflects intra-regional synchronization [40, 41], to compute regional connectivity. To identify regions whose regional connectivity changed significantly after foot-shock experience, we used two-way ANOVA to analyze interaction effects in the results acquired from ReHo. This analysis revealed the ACC to be the region showing the strongest interaction effect among all scanned brain regions in thresholded maps (Fig. 3B) ($n = 10$ for the foot-shock experienced group, $n = 5$ for the naïve group; $P < 0.05$, Student's *t*-test). Further simple effect analysis confirmed that foot-shock experience enhanced the intra-regional connectivity of the ACC (Fig. 3C, D; $P < 0.05$, $n = 10$ for the foot-shock experienced group, $n = 5$ for the NA group, non-parametric rank-sum test). Since altered ReHo is linked with altered neuronal activity [42], these results suggested that the increased social transmission of fear seen in OSs in the EP group may be associated with enhanced neuronal activity in the ACC.

Effects of ACC Lesions on Freezing and Huddling Behavior

To confirm ACC involvement in the social transmission of fear, we asked whether decreasing ACC activity reverses the behavioral phenotypes induced by foot-shock-experience. So, we lesioned the ACC by bilateral delivery of IBO and found a significant decrease in vicarious freezing levels (Fig. 4A, B; $n = 12$ pairs/group, $P < 0.01$, non-parametric rank-sum test), consistent with previous studies [15]. Interestingly, unlike the impaired freezing behavior seen following ACC lesioning, the huddling behavior between DSs and OSs was unaffected (Fig. 4C; $n = 12$ pairs/group, $P = 0.10$, non-parametric rank-sum test). To exclude the possibility that ACC lesioning decreased the expression of fear, we evaluated freezing levels in the classical fear conditioning retrieval period and found no significant difference in primary fear responses between lesioned and control groups (Fig. 4D; $n = 6$/group, $P = 0.4848$, non-parametric rank-sum test). These results indicated that ACC activity specifically affects vicarious freezing but not huddling behaviors during the social transmission of fear.

Ablating the ACC-to-MDL Projection Delays the Onset of Vicarious Behavior

Since the ACC contributes to experience-dependent vicarious freezing, we asked which ACC projections specifically modulate this behavior. To identify regions connected to the ACC, we injected neuron-labeling AAV-hSyn-EGFP

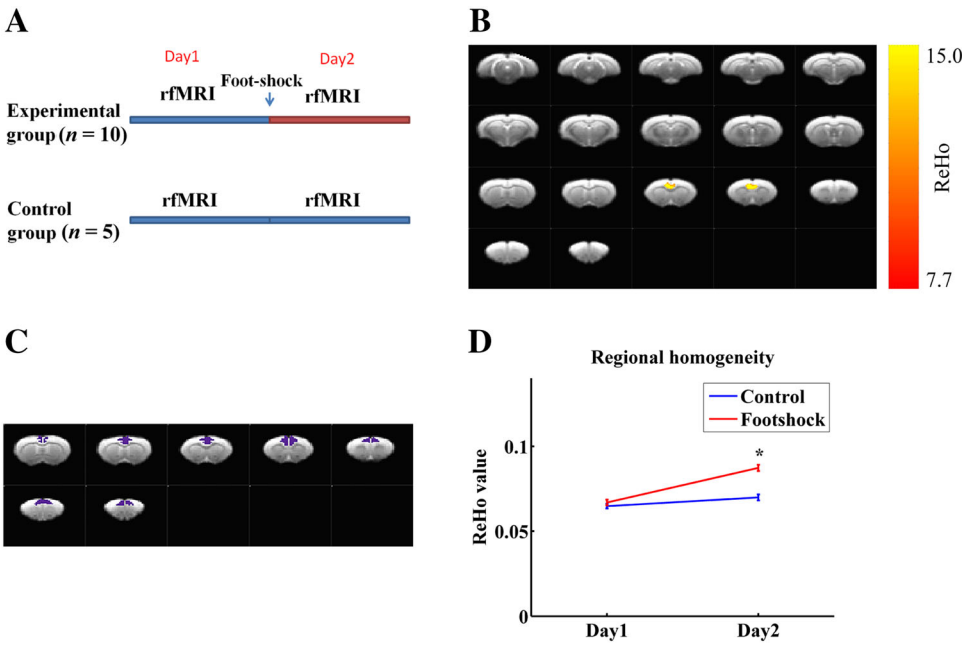

Fig. 3 Foot-shock experience is associated with enhanced regional connectivity in the ACC. **A** Schema of fMRI experimental design. **B** Thresholded maps of interaction effects based on a two-way repeated measures ANOVA. Yellow voxels indicate region with significant interaction effects (corrected $P < 0.05$). **C** The ACC was selected for simple effect analysis; purple voxels indicate the selected regions. **D** Simple effect analysis of the ReHo values in foot-shock-experienced and naïve rats on days 1 and 2. Data are presented as the mean ± SEM; $^{*}P < 0.05$, non-parametric rank-sum test.

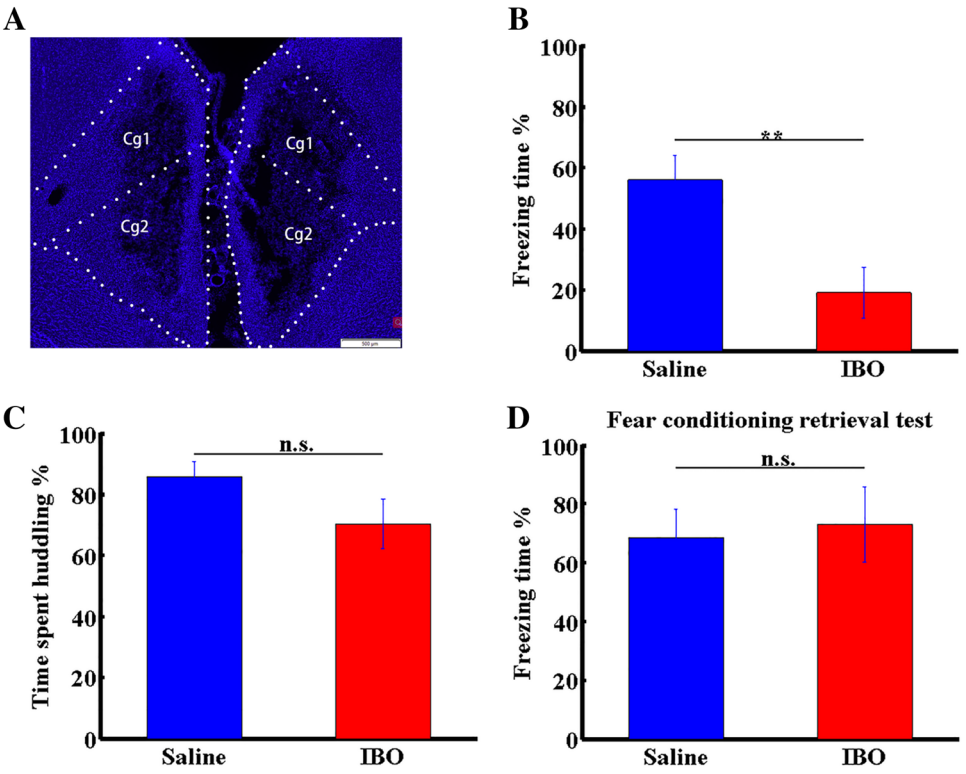

Fig. 4 ACC lesioning impairs vicarious freezing but not huddling behaviors following foot-shock experience. **A** Effects of IBO. Blue represent the nuclei stained with DAPI. Cg1, 2, cingulate cortex 1 and 2. **B**, **C** Percentage freezing (**B**) and huddling (**C**) times of OS rats in IBO- and saline-treated groups. **D** Percentage freezing times of OS rats in IBO- or saline-treated groups in the retrieval period after fear conditioning. Data are presented as the mean ± SEM; $^{**}P < 0.01$, non-parametric rank-sum test, n.s., not significant.

virus into the ACC and observed that the MDL received dense fiber terminal input from the ACC (Fig. 5A). We also injected cholera toxin B into the MDL to retrogradely trace projections and observed dense labeling of ACC cell bodies (Fig. 5B). These results, which are consistent with those of others [15], showed that the MDL receives ACC input. However, the function of these projections remained unclear.

We next investigated the function of the ACC-to-MDL projection using an ablation strategy. We first performed control experiments by injecting retroAAV-Cre into the MDL and AAV-FLEX-tdTomato into the ACC (Fig. 5C),

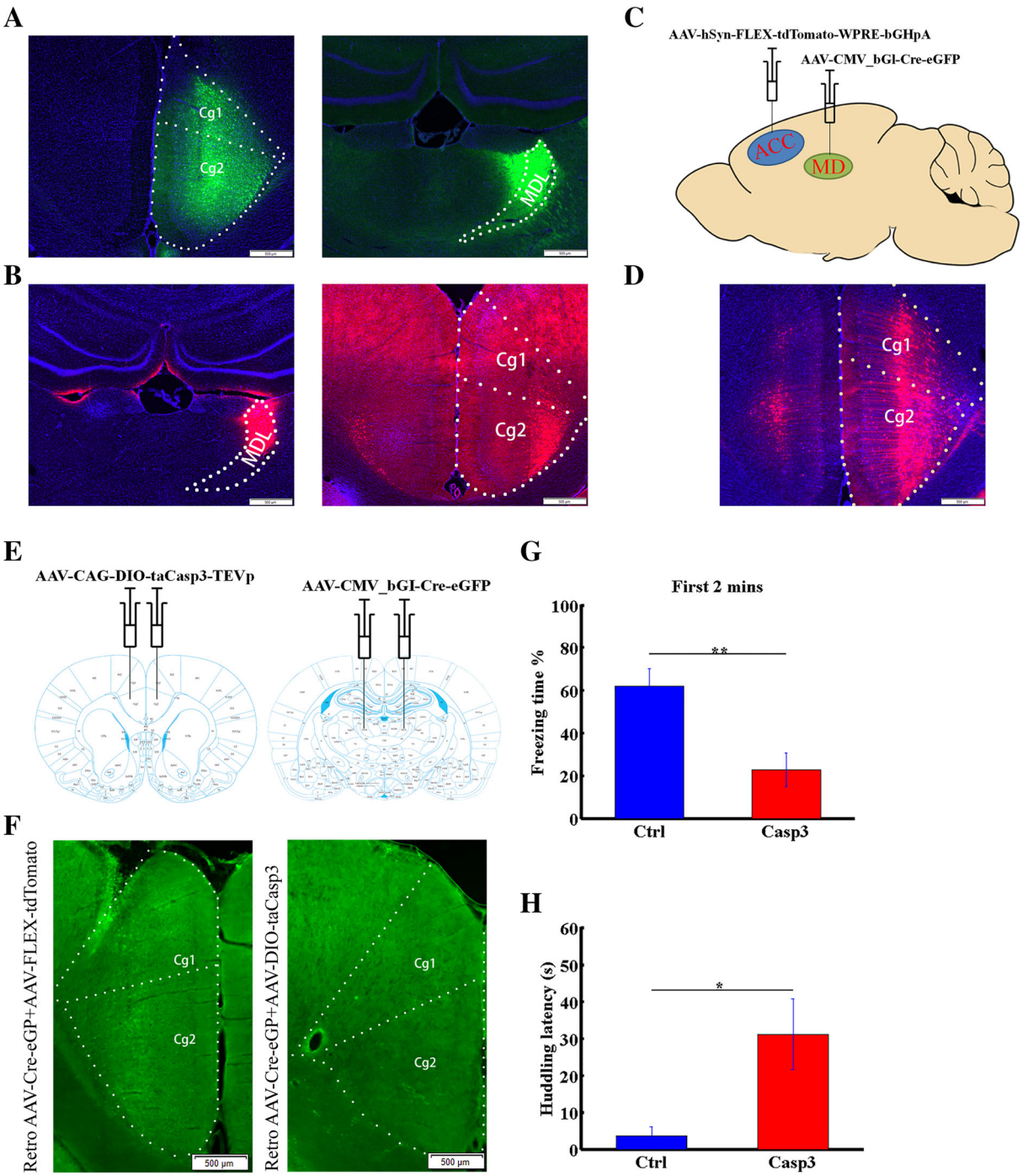

Fig. 5 Ablating ACC neurons projecting to the MDL delays the onset of vicarious behaviors. **A** Left panel, AAV-hSyn-EGFP injection target in the ACC; right panel, labeled projection terminals in the MDL. **B** Left panel, Cholera toxin B injection target in the MDL; right panel, ACC cell bodies. Cg1, 2, cingulate cortex 1 and 2. **C** Diagram of virus-injection strategy used to label MDL-projecting ACC neurons. AAV-hSyn-FLEX-tdTomato-WPRE-bGHpA was injected into the right ACC and AAV-CMV_bGI-Cre-EGFP into the right MDL. **D** ACC neurons projecting to the MDL labeled by the strategy shown in **A**. **E** Diagram of virus-injection strategy used to ablate MDL-projecting ACC neurons. AAV-CAG-DIO-taCasp3-TEVp was injected into the ACC on both sides and AAV-CMV_bGI-Cre-EGFP into the MDL on both sides. **F** Examples of eGFP-labeled neurons in the ACC of control (left) and caspase3 (right) groups. **G** Percentage freezing time in the first 2 min of the test in caspase-3-expressing and control groups. **H** Huddling behavior latency in caspase-3-expressing and control groups. Data are presented as the mean ± SEM; $*P < 0.05$, $**P < 0.01$, non-parametric rank-sum test.

and found that MDL-projecting ACC neurons were effectively labeled by this strategy (Fig. 5D). These results demonstrated that our strategy effectively targeted the ACC-to-MDL projection. We then bilaterally injected a retrograde-labeling virus (retroAAV-CMV_bGl-Cre-eGFP), which carries Cre recombinase, into the MDL and then injected a Cre-dependent anterograde-labeling virus (AAV-CAG-DIO-taCasp3-TEVp), which carries the double-floxed inverted open reading frame (as a substitute for FLEX) and caspase-3 (to induce apoptotic ablation), into the ACC on both sides (Fig. 5E). As the example shows, retroAAV-Cre + AAV-DIO-taCasp3 decreased the number of retro-AAV-Cre-labeled GFP^+ neurons in the ACC (Fig. 5F).

Behavioral tests showed that, for the time of freezing and huddling behaviors throughout the test period, rats in the experimental and control groups performed comparably (data not shown). However, further analysis revealed that ablation of ACC neurons projecting to the MDL decreased the vicarious freezing behavior in OSs in the first 2 min of behavioral testing (Fig. 5G; $n = 8$ pairs for the Casp3 group, $n = 12$ pairs for the control group, $P < 0.01$, non-parametric rank-sum test) and increased the latency of huddling onset (Fig. 5H; $n = 8$ pairs for the Casp3 group, $n = 12$ pairs for the control group, $P < 0.05$, non-parametric rank-sum test). These results demonstrated that ablating the ACC projection to the MDL delays the onset of vicarious behavior.

Activation of the ACC-to-MDL Projection Decreases Vicarious Freezing Behavior

To further assess the role of the ACC-to-MDL projection in the social transmission of fear, we injected AAV virus carrying channelrhodopsin (ChR2) into the right ACC and implanted an optical fiber into the right MDL (Fig. 6A, B). As a control, we injected AAV virus carrying EGFP into the right ACC and implanted an optical fiber into the right MDL (Fig. 6C). To confirm the activation of neurons expressing ChR2 by light, we delivered blue light pulses at two frequencies (1 or 5 Hz) to a brain slice expressing ChR2 and found that ChR2-expressing neurons effectively followed the light pulse stimuli (Fig. 6D), while slices from a control group expressing AAV-EGFP in the ACC did not.

We then asked whether activation of the ACC–MDL projection alters the social transmission of fear. Following application of a continuous train of blue light pulses (473 nm, 20 Hz, 5 mW) to axon terminals in the MDL in the test period, we observed a significant decrease in vicarious freezing behavior in OSs (Fig. 6E). However, the huddling time of DSs and OSs in the EP group was unaffected (Fig. 6F; $n = 8$ pairs for the ChR2 group, $n = 11$ pairs for the control group, $P < 0.01$, non-parametric rank-sum test). To exclude the possibility that these outcomes were due to impaired expression of fear, we measured fear-expression time in the retrieval period after fear conditioning of ChR2- or EGFP-expressing rats and found that the values were comparable (Fig. 6G; $n = 6$ for each EGFP- and ChR2-delivered group, non-parametric rank-sum test). We also asked whether the decreased vicarious freezing was due to enhanced locomotion by monitoring the average locomotor velocity in open field tests. This analysis showed that activation of the ACC-MDL projection did not alter the movement of OSs in the EP group (Fig. 6H; $n = 6$ for each EGFP- and ChR2-delivered group, non-parametric rank-sum test). We concluded that activation of the ACC-to-MDL projection specifically decreases vicarious freezing behavior.

Discussion

In this study, we focused on foot-shock-experienced vicarious freezing behavior and defined the neuronal substrates underlying this behavior. As in humans, experience can modulate the social transmission of fear in rodents (Fig. 2B, C) [43]. Using a paradigm modified from a study by Kim *et al.* [20], we found that an elevated fear state in the DS significantly enhanced the OS fear state, especially vicarious freezing behavior. Using rs-fMRI analysis, we found that ACC regional connectivity was significantly enhanced after foot-shock experience (Fig. 3D). ACC lesioning decreased the vicarious freezing behavior in foot-shock-experienced OSs (Fig. 4B). Given that a previous study reported that an altered ReHo is linked to altered spontaneous neuronal activity [42], and that Zhuo [44] showed that the plasticity of ACC neurons is altered by pain experience in rats and mice, we propose that foot-shock experience alters neuronal plasticity of the ACC, in turn modulating vicarious social behavior. Recent studies have identified a projection from the ACC to the MDL [15, 45], but its function remained unclear. Interestingly, we found that ablation of this projection delayed and its activation decreased vicarious freezing behavior (Figs. 5G, H, and 6E), demonstrating that the ACC modulates vicarious freezing behavior through this projection.

The social transmission of fear, defined as the transfer of fear emotion between individuals, is a primary form of empathy behavior and has been demonstrated in rodents [11]. This ability has been proposed to assist species to cooperatively achieve a common goal [1]. Previous studies have suggested that the transfer of fear is modulated by factors as varied as gender, age, familiarity, experience, and genetic background [10, 11, 25, 46]. In laboratory-bred

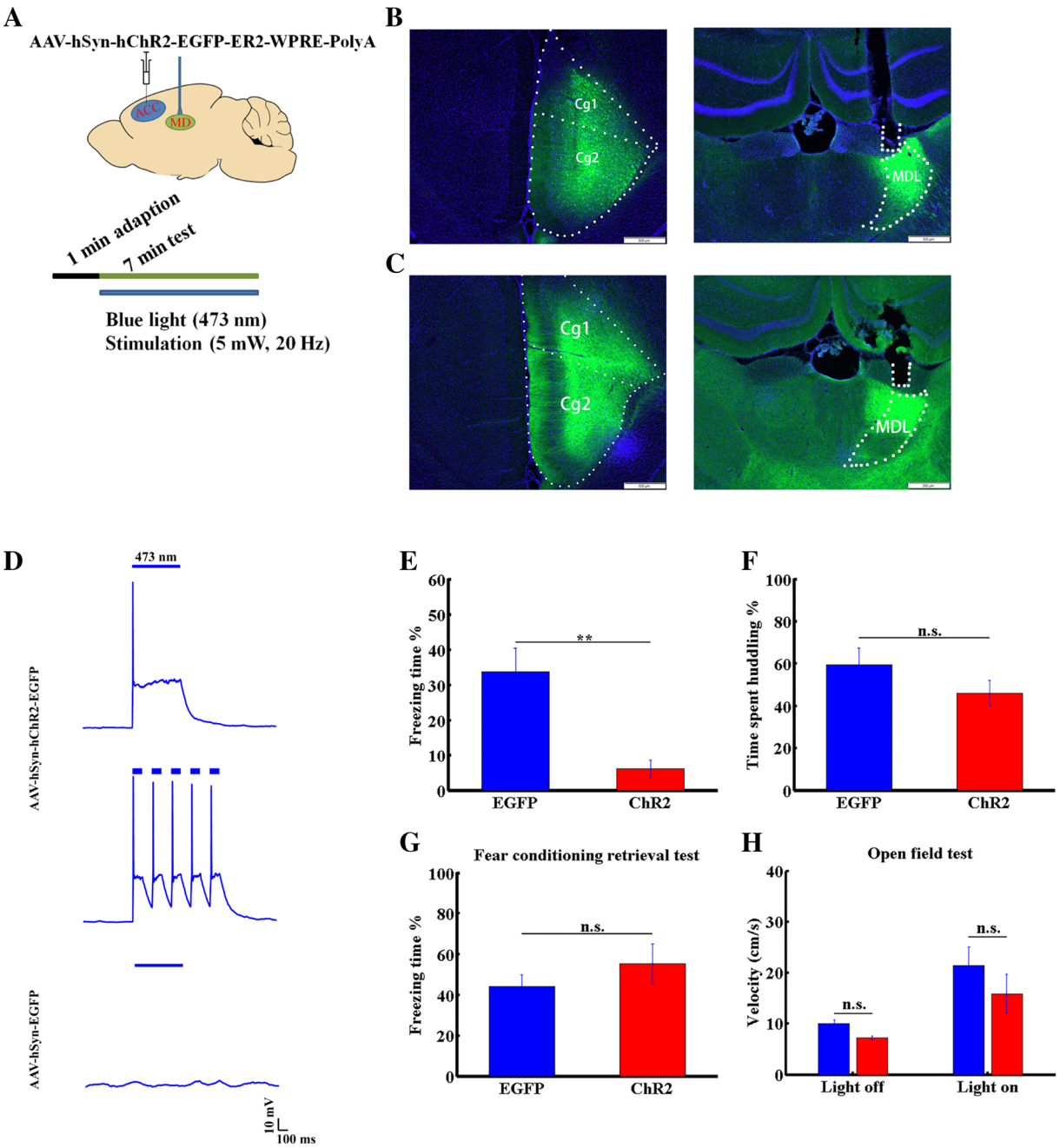

Fig. 6 Activation of the ACC-to-MDL projection decreases vicarious freezing behavior. **A** Diagram showing optogenetic manipulation. **B** Tracing of projection from the ACC to the MDL. Left panel, AAV-hSyn-EGFP virus injection target in the ACC. Cg1, 2, cingulate cortex 1 and 2; right panel, projection terminals and optical fiber position in the MDL. **C** Left panel, AAV-hSyn-hChR2-EGFP virus injection target in the ACC; right panel, projection terminals and optical fiber position in the MDL. Nuclei stained with DAPI. **D** Light pulse-induced response of ChR2-expressing (upper and middle, 10 mW, 1 Hz and 5 Hz, respectively) and EGFP-expressing (lower, 10 mW, 1 Hz) ACC neurons in brain slice. **E**, **F** Freezing (**E**) and huddling (**F**) times of OSs in AAV-hSyn-EGFP (blue) or AAV-hSyn-ChR2 (red) groups. **G** Percentage freezing time of OSs in AAV-hSyn-EGFP- and AAV-hSyn-ChR2-injected groups in the retrieval period after fear conditioning. **H** Locomotor velocity of OSs in AAV-hSyn-EGFP (blue) and AAV-hSyn-ChR2 (red) groups, before and after light stimulation. Data are presented as the mean ± SEM; $^{**}P < 0.01$, non-parametric rank-sum test, n.s., not significant.

rodents, the lack of predators or challenging environments may be associated with lower levels of empathy in response to the distress of conspecifics. For example, when we applied the paradigm of Kim *et al*. [20], we observed unstable performance of OSs (Fig. 2C), possibly due to different breeding or experimental environments. We then determined that this outcome was likely due to the low expression of fear by DSs in the retrieval period, as only 5

of 12 DSs exhibited a freezing response. Thus, we added an extra fear conditioning training session for DSs and allowed OSs to experience foot-shock before the test session. These modifications resulted in more robust vicarious freezing behavior by OSs (Fig. 2H) and allowed us to evaluate the social transmission of fear. Our modified paradigm can serve as a useful tool for future studies of the mechanisms underlying emotion contagion.

Observational fear studies [11] have reported that naïve OS mice show vicarious freezing behavior in response to behavior by DSs. However, we did not observe such behavior by OS rats in the NA group. Similarly, in some mouse studies, naïve OSs display significant observational fear [11], while in others, investigators have searched for but not found these behaviors [19]. Such differences may be due to variable breeding or test environments. Activation or inactivation of the ACC or of somatostatin-positive neurons found in that region [21] bidirectionally modulates the vicarious freezing behavior of OSs. Pain experience can change ACC neuronal plasticity [44], and using ReHo analysis we also found that ACC regional connectivity significantly increased after foot-shock experience (Fig. 3D). These findings suggest overall that vicarious freezing behavior is likely modified by the baseline ACC activity. Moreover, we found that lesioning of the ACC decreased vicarious freezing behavior due to foot-shock experience (Fig. 4B). However, the mechanisms underlying these outcomes need to be examined in greater detail at the neuronal and circuit levels.

Previous studies have shown that the MD participates in the processes of observational fear learning [15] and fear memory retrieval [47]. In addition, the functional connection between the mPFC (which is close to the ACC and overlaps with the dorsal ACC) and the MD is vital for working memory [27], cognitive flexibility [29, 30, 32], attentional control [48], goal-directed behavior [49], and schizophrenia [34, 35]. Recent studies of neuronal circuit-tracing have reported a projection from the ACC to the MDL in mice [45]. Here, we confirmed the existence of this projection in rats and investigated its function. Ablation of ACC neurons projecting to the MDL delayed the onset of vicarious behaviors (Fig. 5G, H). Moreover, activation of ACC projections to the MDL during the test period (Fig. 6E) specifically decreased the vicarious freezing behavior of OSs but not huddling (Fig. 6F) or conditioned fear (Fig. 6G). Based on the results that the mPFC-to-MD circuit is crucial for cognitive flexibility [29, 30, 32], and the MD is involved in fear memory retrieval [47], we propose that ACC neurons projecting to the MDL detect the emotional states of conspecifics and fire in a specific pattern to retrieve the foot-shock-experience-induced fear memory of OSs in the context of DS freezing. Using the Yerkes–Dodson law [50] as reference, in which both hypo- and hyperarousal states in animals can compromise the normal behavioral response, the degree of activation of ACC neurons projecting to the MDL may have an inverted-U influence [51] on vicarious freezing performance. An inverted-U influence in regard to working memory has been reported in another study [52]. In addition, a previous study [53] also found that either activation or inhibition of a specific cell type in the mPFC has an inhibitory effect on performance in a working memory task. Thus, in our experiment, both ablation and over-activation of MDL-projecting ACC neurons probably perturbed the appropriate reaction of downstream neurons in the physiological state, and then resulted in an impairment of vicarious freezing behavior.

Recent studies have reported that the brain oxytocin system modulates empathy in humans and rodents [25, 54, 55], and specifically, intranasal oxytocin administration enhances observational fear in mice [25]. Interestingly, the oxytocin receptor is expressed in what are likely to be interneurons of the ACC [56, 57]. Future studies are needed to address whether neurons expressing oxytocin receptors and ACC projection neurons function together to modulate vicarious behavior.

Limitations

In the present study, we used rs-fMRI to screen the brain regions that are correlated with experience-dependent vicarious freezing behavior. We performed rs-fMRI screening on anesthetized rats, and behavioral assays on freely-moving rats. We found that foot-shock not only increased the regional connectivity of the ACC, but also the performance of vicarious freezing. However, we did not provide sufficient evidence to support a causal relation between the changes in the regional connectivity of the ACC and the increased vicarious freezing behavior. In terms of the pharmacological lesion, caspase3 ablation, and optogenetic manipulation experiments, we just tested limited behavioral tasks. In addition, the ACC is a sophisticated brain region associated with various functions. Thus, we cannot exclude the possibility that other behaviors could have been affected by these manipulations.

Conclusions

In summary, we modified a previous paradigm of social transmission of fear and found that foot-shock experience enhanced vicarious behavior and was associated with enhanced regional connectivity of the ACC. Activation or ablation of the ACC-to-MDL projection specifically decreased the vicarious freezing behavior, suggesting that these neurons fire in a specific pattern to modulate these

behaviors. Our findings provide a mechanistic understanding of foot-shock-experienced vicarious freezing behavior and new clues for future studies of the mechanisms underlying more advanced empathy behaviors.

Acknowledgements We thank Dr. Dingcheng Wu for help in data analysis. We are also grateful for technical support from the Optical Imaging Facility and the Animal Facility of the Institute of Neuroscience, Chinese Academy of Sciences. This work was supported in part by The National Key Research and Development Program of China (2017YFB1300200, 2017YFB1300203) and the National Natural Science Foundation of China (61627808).

Conflict of interest The authors declare that the research was conducted in the absence of any commercial or financial relationship that could be construed as a potential conflict of interest.

References

1. de Waal FBM, Preston SD. Mammalian empathy: behavioural manifestations and neural basis. Nat Rev Neurosci 2017, 18: 498–509.
2. Frith U, Happe F. Autism spectrum disorder. Curr Biol 2005, 15: R786–790.
3. Baron-Cohen S, Ashwin E, Ashwin C, Tavassoli T, Chakrabarti B. Talent in autism: hyper-systemizing, hyper-attention to detail and sensory hypersensitivity. Philos Trans R Soc Lond B Biol Sci 2009, 364: 1377–1383.
4. Achim AM, Ouellet R, Roy MA, Jackson PL. Assessment of empathy in first-episode psychosis and meta-analytic comparison with previous studies in schizophrenia. Psychiatry Res 2011, 190: 3–8.
5. Horan WP, Reise SP, Kern RS, Lee J, Penn DL, Green MF. Structure and correlates of self-reported empathy in schizophrenia. J Psychiatr Res 2015, 66-67: 60–66.
6. Derntl B, Finkelmeyer A, Toygar TK, Hulsmann A, Schneider F, Falkenberg DI, *et al.* Generalized deficit in all core components of empathy in schizophrenia. Schizophrenia Res 2009, 108: 197–206.
7. de Waal FBM. Putting the altruism back into altruism: The evolution of empathy. Annu Rev Psychol 2008, 59: 279–300.
8. Zaki J, Ochsner K. The neuroscience of empathy: progress, pitfalls and promise. Nat Neurosci 2012, 15: 675–680.
9. Decety J. The neuroevolution of empathy. Ann N Y Acad Sci 2011, 1231: 35–45.
10. Chen Q, Panksepp JB, Lahvis GP. Empathy is moderated by genetic background in mice. PLoS One 2009, 4: e4387.
11. Jeon D, Kim S, Chetana M, Jo D, Ruley HE, Lin SY, *et al.* Observational fear learning involves affective pain system and Cav1.2 Ca^{2+} channels in ACC. Nat Neurosci 2010, 13: 482–488.
12. Sivaselvachandran S, Acland EL, Abdallah S, Martin LJ. Behavioral and mechanistic insight into rodent empathy. Neurosci Biobehav Rev 2018, 91: 130–137.
13. Chen J. Empathy for distress in humans and rodents. Neurosci Bull 2018, 34: 216–236.
14. Liddle MJ, Bradley BS, McGrath A. Baby empathy: infant distress and peer prosocial responses. Infant Ment Health J 2015, 36: 446–458.
15. Kim S, Matyas F, Lee S, Acsady L, Shin HS. Lateralization of observational fear learning at the cortical but not thalamic level in mice. Proc Natl Acad Sci U S A 2012, 109: 15497–15501.
16. Twining RC, Vantrease JE, Love S, Padival M, Rosenkranz JA. An intra-amygdala circuit specifically regulates social fear learning. Nat Neurosci 2017, 20: 459–469.
17. Guzman YF, Tronson NC, Guedea A, Huh KH, Gao C, Radulovic J. Social modeling of conditioned fear in mice by non–fearful conspecifics. Behav Brain Res 2009, 201: 173–178.
18. D'Amato FR. Kin interaction enhances morphine analgesia in male mice. Behav Pharmacol 1998, 9: 369–373.
19. Allsop SA, Wichmann R, Mills F, Burgos-Robles A, Chang CJ, Felix-Ortiz AC, *et al.* Corticoamygdala transfer of socially derived information gates observational learning. Cell 2018, 173: 1329-1342 e1318.
20. Kim EJ, Kim ES, Covey E, Kim JJ. Social transmission of fear in rats: the role of 22-kHz ultrasonic distress vocalization. PLoS One 2010, 5: e15077.
21. Keum S, Kim A, Shin JJ, Kim JH, Park J, Shin HS. A missense variant at the Nrxn3 locus enhances empathy fear in the mouse. Neuron 2018, 98: 588–601.e585.
22. Hurlemann R, Patin A, Onur OA, Cohen MX, Baumgartner T, Metzler S, *et al.* Oxytocin enhances amygdala-dependent, socially reinforced learning and emotional empathy in humans. J Neurosci 2010, 30: 4999–5007.
23. Kovacs B, Keri S. Off-label intranasal oxytocin use in adults is associated with increased amygdala-cingulate resting-state connectivity. Eur Psychiatry 2015, 30: 542–547.
24. Meyer-Lindenberg A, Domes G, Kirsch P, Heinrichs M. Oxytocin and vasopressin in the human brain: social neuropeptides for translational medicine. Nat Rev Neurosci 2011, 12: 524–538.
25. Pisansky MT, Hanson LR, Gottesman, II, Gewirtz JC. Oxytocin enhances observational fear in mice. Nat Commun 2017, 8: 2102.
26. Bernhardt BC, Singer T. The neural basis of empathy. Annu Rev Neurosci 2012, 35: 1–23.
27. Bolkan SS, Stujenske JM, Parnaudeau S, Spellman TJ, Rauffenbart C, Abbas AI, *et al.* Thalamic projections sustain prefrontal activity during working memory maintenance. Nat Neurosci 2017, 20: 987–996.
28. Cardoso-Cruz H, Sousa M, Vieira JB, Lima D, Galhardo V. Prefrontal cortex and mediodorsal thalamus reduced connectivity is associated with spatial working memory impairment in rats with inflammatory pain. Pain 2013, 154: 2397–2406.
29. Rikhye RV, Gilra A, Halassa MM. Thalamic regulation of switching between cortical representations enables cognitive flexibility. Nat Neurosci 2018, 21: 1753–1763.
30. Marton TF, Seifikar H, Luongo FJ, Lee AT, Sohal VS. Roles of prefrontal cortex and mediodorsal thalamus in task engagement and behavioral flexibility. J Neurosci 2018, 38: 2569–2578.
31. Jett JD, Bulin SE, Hatherall LC, McCartney CM, Morilak DA. Deficits in cognitive flexibility induced by chronic unpredictable stress are associated with impaired glutamate neurotransmission in the rat medial prefrontal cortex. Neuroscience 2017, 346: 284–297.
32. Parnaudeau S, Taylor K, Bolkan SS, Ward RD, Balsam PD, Kellendonk C. Mediodorsal thalamus hypofunction impairs flexible goal-directed behavior. Biol Psychiatry 2015, 77: 445–453.
33. Anticevic A, Cole MW, Repovs G, Murray JD, Brumbaugh MS, Winkler AM, *et al.* Characterizing thalamo-cortical disturbances in schizophrenia and bipolar illness. Cereb Cortex 2014, 24: 3116–3130.
34. Woodward ND, Karbasforoushan H, Heckers S. Thalamocortical dysconnectivity in schizophrenia. Am J Psychiatry 2012, 169: 1092–1099.
35. Anticevic A, Haut K, Murray JD, Repovs G, Yang GJ, Diehl C, *et al.* Association of thalamic dysconnectivity and conversion to psychosis in youth and young adults at elevated clinical risk. JAMA Psychiatry 2015, 72: 882–891.

36. Zhou Y, Fan L, Qiu C, Jiang T. Prefrontal cortex and the dysconnectivity hypothesis of schizophrenia. Neurosci Bull 2015, 31: 207–219.
37. Valdes-Hernandez PA, Sumiyoshi A, Nonaka H, Haga R, Aubert-Vasquez E, Ogawa T, *et al.* An *in vivo* MRI template set for morphometry, tissue segmentation, and fMRI localization in rats. Front Neuroinform 2011, 5: 26.
38. Zang Y, Jiang T, Lu Y, He Y, Tian L. Regional homogeneity approach to fMRI data analysis. Neuroimage 2004, 22: 394–400.
39. Song XW, Dong ZY, Long XY, Li SF, Zuo XN, Zhu CZ, *et al.* REST: a toolkit for resting-state functional magnetic resonance imaging data processing. PLoS One 2011, 6: e25031.
40. Wu T, Grandjean J, Bosshard SC, Rudin M, Reutens D, Jiang T. Altered regional connectivity reflecting effects of different anaesthesia protocols in the mouse brain. Neuroimage 2017, 149: 190–199.
41. Yin Y, Jin CF, Eyler LT, Jin H, Hu XL, Duan L, *et al.* Altered regional homogeneity in post-traumatic stress disorder: a restingstate functional magnetic resonance imaging study. Neurosci Bull 2012, 28: 541–549.
42. Peng CY, Chen YC, Cui Y, Zhao DL, Jiao Y, Tang TY, *et al.* Regional coherence alterations revealed by resting-state fMRI in post-stroke patients with cognitive dysfunction. PLoS One 2016, 11: e0159574.
43. Atsak P, Orre M, Bakker P, Cerliani L, Roozendaal B, Gazzola V, *et al.* Experience modulates vicarious freezing in rats: a model for empathy. PLoS One 2011, 6: e21855.
44. Zhuo M. Long-term potentiation in the anterior cingulate cortex and chronic pain. Philos Trans R Soc Lond B Biol Sci 2014, 369: 20130146.
45. Matyas F, Lee J, Shin HS, Acsady L. The fear circuit of the mouse forebrain: connections between the mediodorsal thalamus, frontal cortices and basolateral amygdala. Eur J Neurosci 2014, 39: 1810–1823.
46. Sanders J, Mayford M, Jeste D. Empathic fear responses in mice are triggered by recognition of a shared experience. PLoS One 2013, 8: e74609.
47. Padilla-Coreano N, Do-Monte FH, Quirk GJ. A time-dependent role of midline thalamic nuclei in the retrieval of fear memory. Neuropharmacology 2012, 62: 457–463.
48. Schmitt LI, Wimmer RD, Nakajima M, Happ M, Mofakham S, Halassa MM. Thalamic amplification of cortical connectivity sustains attentional control. Nature 2017, 545: 219–223.
49. Alcaraz F, Fresno V, Marchand AR, Kremer EJ, Coutureau E, Wolff M. Thalamocortical and corticothalamic pathways differentially contribute to goal-directed behaviors in the rat. Elife 2018, 7.
50. Yerkes RM, Dodson JD. The relation of strength of stimulus to rapidity of habit-formation. J Comp Neurol Psychol 1908, 18: 459–482.
51. Arnsten AF, Wang MJ, Paspalas CD. Neuromodulation of thought: flexibilities and vulnerabilities in prefrontal cortical network synapses. Neuron 2012, 76: 223–239.
52. Arnsten AF, Cai JX, Murphy BL, Goldman-Rakic PS. Dopamine D1 receptor mechanisms in the cognitive performance of young adult and aged monkeys. Psychopharmacology (Berl) 1994, 116: 143–151.
53. Liu D, Gu XW, Zhu J, Zhang XX, Han Z, Yan WJ, *et al.* Medial prefrontal activity during delay period contributes to learning of a working memory task. Science 2014, 346: 458–463.
54. Barraza JA, Zak PJ. Empathy toward strangers triggers oxytocin release and subsequent generosity. Ann N Y Acad Sci 2009, 1167: 182–189.
55. Riem MM, Bakermans-Kranenburg MJ, Pieper S, Tops M, Boksem MA, Vermeiren RR, *et al.* Oxytocin modulates amygdala, insula, and inferior frontal gyrus responses to infant crying: a randomized controlled trial. Biol Psychiatry 2011, 70: 291–297.
56. Mitre M, Marlin BJ, Schiavo JK, Morina E, Norden SE, Hackett TA, *et al.* A distributed network for social cognition enriched for oxytocin receptors. J Neurosci 2016, 36: 2517–2535.
57. Li K, Nakajima M, Ibanez-Tallon I, Heintz N. A cortical circuit for sexually dimorphic oxytocin-dependent anxiety behaviors. Cell 2016, 167: 60–72 e11.